IEEE *Access*
Multidisciplinary : Rapid Review : Open Access Journal

Natural graphite sheet heat sinks with embedded heat pipes

MARTIN CERMAK[1], XAVIER FAURE[1,2], ALI SAKET[3],(Student Member, IEEE), MAJID BAHRAMI[1], MARTIN ORDONEZ[3],(Fellow, IEEE)

[1]Laboratory for Alternative Energy Conversion, School of Mechatronic Systems Engineering, Simon Fraser University, 250-13450 102 Avenue, Surrey, British Columbia, V3T 0A3, Canada
[2]The Institut National des Sciences Appliquées de Lyon, 20 avenue Albert Einstein, 69621, Villeurbanne cedex, France
[3]Electrical and Computer Engineering Department, The University of British Columbia, 2332 Main Mall, Vancouver, British Columbia, V6T 1Z4, Canada

Corresponding author: Majid Bahrami (email: mbahrami@sfu.ca ; tel.: +1 (778) 782-8538).

ABSTRACT Natural graphite sheet (NGS) is a candidate material for lightweight, high-performance heat sinks. We show that the low through–plane thermal conductivity can be mitigated by using heat pipes. In the measured configuration, the thermal resistance of an NGS heat sink with embedded heat pipes is comparable to that of a geometrically-identical aluminum one. The achieved weight reduction is 37 %. When electrical insulation of a heat sink is not required, soft and conforming NGS does not require thermal grease at the interface between the heat source and the heat sink. The low electrical conductivity of NGS does not lead to a decrease in common mode conducted emissions, but the potential to reduce the radiated emissions was quantified to be 12 to 97 % based on an analogy with antennas. In practical applications, replacing an existing heat sink with a geometrically identical NGS one is not recommended because it limits the achievable improvements in thermal performance, weight, and cost. Instead, we suggest using an optimization algorithm to determine the optimal heat sink geometry.

INDEX TERMS Aerospace materials, Carbon, Circuit noise, Conducted emissions, Electromagnetic compliance, Electromagnetic interference, Electronics cooling, Graphite, Heat sinks, Radiated emissions, Thermal management of electronics, Electronic packaging, Thermal management

I. INTRODUCTION

HEAT sinks are used to transfer heat from heat-generating electronic components into the surrounding air. Their primary role is to prevent a temperature-related failure of the components. Selecting a suitable heat sink for a given application is a trade-off between the thermal performance, cost, weight, size, reliability, acoustic noise, and electromagnetic emissions.

The most widespread heat sink materials are aluminum and copper, where the latter offers higher thermal conductivity, but comes with a cost and weight penalty. Natural graphite sheet (NGS) is a material whose properties are in line with the heat sink requirements. Over the practical range of densities 0.5 to 1.7 g·cm^{-3} the weight of NGS is 19 to 70 % of aluminum, and 6 to 21 % of copper. The comparison of cost is limited by the low maturity of the NGS supply chain; however, based on the raw material market summary in [1], the cost-per-volume of NGS for the above range of densities

is 7 to 25 % of aluminum, and 1 to 3 % of copper. The material properties of NGS are highly anisotropic, density dependent, and some change with compression [2]. The thermal conductivity is 100 to 350 W·m^{-1}·K^{-1} in the in–plane direction and 2 to 5 W·m^{-1}·K^{-1} in the through–plane direction. Graphite is stable in temperatures up to 600 °C [3] and shows good corrosion resistance [4]. A graphical comparison of NGS with aluminum and copper is given in Figure 1.

The concept of using NGS for building heat sinks was first proposed for server cooling in the work by Chen et al. [7] and Marotta et al. [8]. The authors concluded that the low through–plane thermal conductivity limits the thermal performance, especially in cases when the heat source covers only a small portion of the base. Issues with mounting due to the low mechanical strength of NGS were reported. To address the drawbacks, the authors abandoned the concept of all-NGS heat sinks and moved to hybrid ones with copper
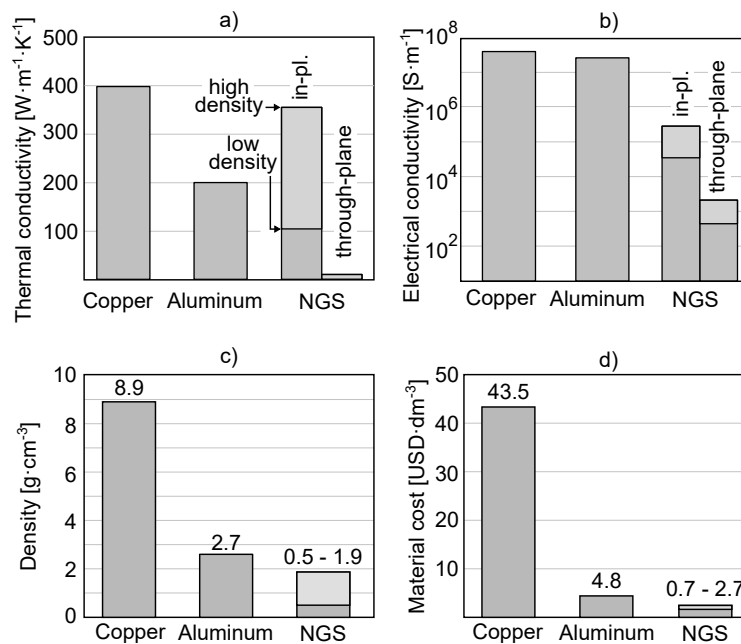
FIGURE 1. A comparison of a) thermal conductivity, b) electrical conductivity, c) density, and d) material cost of NGS, aluminum, and copper.

base and NGS fins. General conclusions about the feasibility of NGS heat sinks cannot be made based on the two articles.

Icoz and Arik [9] considered a material with properties similar to a high-density NGS in their study of lightweight heat sinks for natural convection applications. They concluded that, based on their figure of merit quantity $1/(mR_{th})$ (where m is the weight and R_th is the thermal resistance), carbon foam performs three times better than NGS, aluminum, and plastic with thermally conductive additives. The thermal resistance of the NGS, aluminum, and carbon foam heat sinks was comparable. Low-density NGS was not considered, which renders any conclusions on NGS incomplete. Other feasibility factors such as cost were not considered in the comparison.

The limited coverage of NGS heat sinks in the literature is contrary to their potential. Existing manufacturing methods are capable of forming NGS into complex shapes thus allowing heat sink geometries that were previously cost-prohibitive or impossible. The low material cost increases the chances of successful commercialization, and the low electrical conductivity can lead to lower electromagnetic emissions. The high in–plane thermal conductivity is attractive, but the understanding of the limitations arising from the low through–plane thermal conductivity is incomplete.

In our previous work [10], [11], we built and tested staggered plate fin NGS heat sinks and showed that when the heat sink width is comparable to the heat source size, their thermal resistance is comparable to geometrically identical aluminum ones with thermal grease applied at the device-sink interface. A detailed analysis revealed that soft NGS conforms to micro-roughness and out-of-flatness of the heat source, which reduces the TCR at the device-sink interface,

and in turn eliminates the need for a thermal grease.

In this study, we extend the focus to large heat sinks whose size in the through–plane NGS direction is multiple times larger than the heat source size. For such heat sinks the low through–plane thermal conductivity is expected to degrade the thermal performance. Furthermore, we investigate the effect of electrical insulation, and the potential to reduce the electromagnetic emission of power electronics by using NGS heat sinks. The published literature contains studies on using electrically insulative heat sink materials to decrease both conducted [12] and radiated emission [13]. However, a study on the effect of using a lossy electrical conductor is missing, and we aim to fill the gap by considering the specific case of NGS.

The work presented here comprises an intermediate step toward evaluating the feasibility of NGS heat sinks for power electronics applications. The objectives are to: i) experimentally evaluate the thermal performance of large, geometrically identical heat sinks manufactured from NGS and aluminum, ii) investigate the possibility of embedding heat pipes into NGS heat sinks to enhance the heat conduction in the through–plane direction, iii) investigate the effect of NGS heat sinks on conducted and radiated emissions in power electronics, and iv) interpret the results in terms of the feasibility of NGS heat sinks.

II. METHODOLOGY

Fig. 2 shows the three heat sinks used for the present study: i) reference CNC-machined 6061 aluminum heat sink (AL), ii) NGS heat sink with aligning plastic rods in the base (NGS), and iii) NGS heat sink with two 4 mm diameter U shape heat pipes (NGS+HP). All the heat sinks have 42 fins, and the tar-
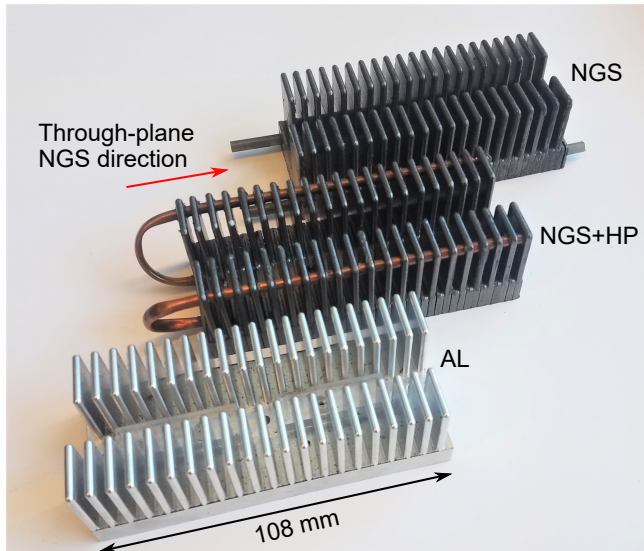
IEEE Access

FIGURE 2. Three heat sinks used in this study: reference aluminum heat sink (AL), natural graphite sheet heat sink (NGS), and natural graphite sheet heat sink with embedded heat pipes (NGS+HP). The through–plane direction of NGS is shown by the red arrow; the in–plane directions are perpendicular to the through–plane direction.

get dimensions were 50.8 mm width, 34.1 mm height, 117.6 mm length, and 2.8 mm fin thickness. Both NGS heat sinks were prepared from a 1 g cm^{-3} sheet, which corresponds to the in–plane thermal conductivity of 190 W·m^{-1}·K^{-1}, through–plane thermal conductivity of 4 W·m^{-1}·K^{-1}, in–plane electrical conductivity of 974 S·cm^{-1}, and through–plane electrical conductivity of 11 S·cm^{-1}. To improve machinability—which was required for drilling the holes for heat pipes—the NGS was polymer impregnated (Hernon HPS 991). The heat sink geometry was selected with respect to the constrained ability to manufacture the NGS prototypes. As a result, the thermal performance is not optimal.

The test setup for the thermal measurements consisted of an acrylic frame with two axial 40 mm diameter fans (JMC 3503 4028-12) in an impinging flow configuration as shown in Fig. 3a. The fans were driven by a 5 V power supply and they were kept aligned with the heat sink by the mounting rods that fit into the holes in the base of the heat sinks. The considered heat generating semiconductor device was an IXYS DSEI 30-06A diode. It was attached to the heat sink with an M3 bolt, but since tapping threads in NGS is not possible, an acrylic pressure spreader with an M3 nut was installed between the fins on the other side of the base. The bolt was tightened using the CDI 151NSM torque screwdriver set to 0.2 Nm, which translates to the contact pressure of 1 MPa. A Chroma 62012P-40-120 programmable DC power supply kept a constant 15 A current through the device, which translated to the dissipated heat flow $\dot{Q}$ of approximately 16 W. Three Omega 5SRTC T-type 36 AWG thermocouples were used to monitor the temperature of the device T_D, heat sink T_S, and inlet ambient air T_A. The heat sink thermocouple was attached by aluminum tape at the

location shown in Fig. 3b, and the installation of the device thermocouple was described in [11]. The thermal performance was quantified by evaluating the thermal resistances as:

$$R_{th,DS} = \frac{T_D - T_S}{\dot{Q}}, \quad (1)$$

$$R_{th,SA} = \frac{T_S - T_A}{\dot{Q}}, \quad (2)$$

$$R_{th,DA} = \frac{T_D - T_A}{\dot{Q}}, \quad (3)$$

where $R_{th,DS}$ is the device-to-sink thermal resistance, $R_{th,SA}$ is the sink-to-ambient thermal resistance, and $R_{th,DA}$ is the total device-to-ambient thermal resistance.

To quantify the potential reduction of common mode conducted emissions, the impedance of the corresponding current path was measured using a Keysight E4990A Impedance analyzer with a 42941A probe as shown in Fig. 3b. For the typical case of grounded insulated heat sinks, the common mode currents flow in a loop whose equivalent circuit (Fig. 3c) consists of the capacitor C_{DS} formed by the electrical insulation between the device and the heat sink, resistance and inductance of the heat sink R_{HS} and L_{HS}, impedance of the ground coupling Z_G whose magnitude is dependent on the system, and the voltage excitation V_{EX} that arises from the switching operation of the device. The effect of the heat sink material was evaluated by comparing the impedance between points D and G, as shown in Figure 3d. The low electrical conductivity of NGS was expected to results in high R_{HS}, which increases the total impedance of the common mode loop, and thus decreases the common mode currents.

For both the thermal and impedance studies, three cases shown in Fig. 4 were considered. In the non-insulated case (Fig. 4a), the device was mounted directly on the heat sink, while in the two insulated cases (Fig. 4b and 4c) a 0.07 mm thick adhesive coated polyimide film (Nitto P-221) and a 1.6 mm thick Al$_2$O$_3$ pad (Aavid 4169G) were used. In the thermal study, an additional measurement of the non-insulated case with the Thermalcote 251 thermal grease was carried out to show the effect of TCR at the device-sink interface.

The additional measurement details can be found in [14]. The raw data files, data processing implementation, uncertainty analysis, additional photographs, and the CAD model of the heat sink geometry can be accessed in [15].

III. RESULTS
A. THERMAL PERFORMANCE
The results of the thermal measurements are summarized in Fig. 5. The total device-to-ambient thermal resistance $R_{th,DA}$ given by the total height of the bars has been split into the device-to-sink thermal resistance $R_{th,DS}$ (orange) and sink-to-ambient thermal resistance $R_{th,SA}$ (blue). $R_{th,DS}$ includes the resistances arising from the device package, device-to-sink interface, and electrical insulation.
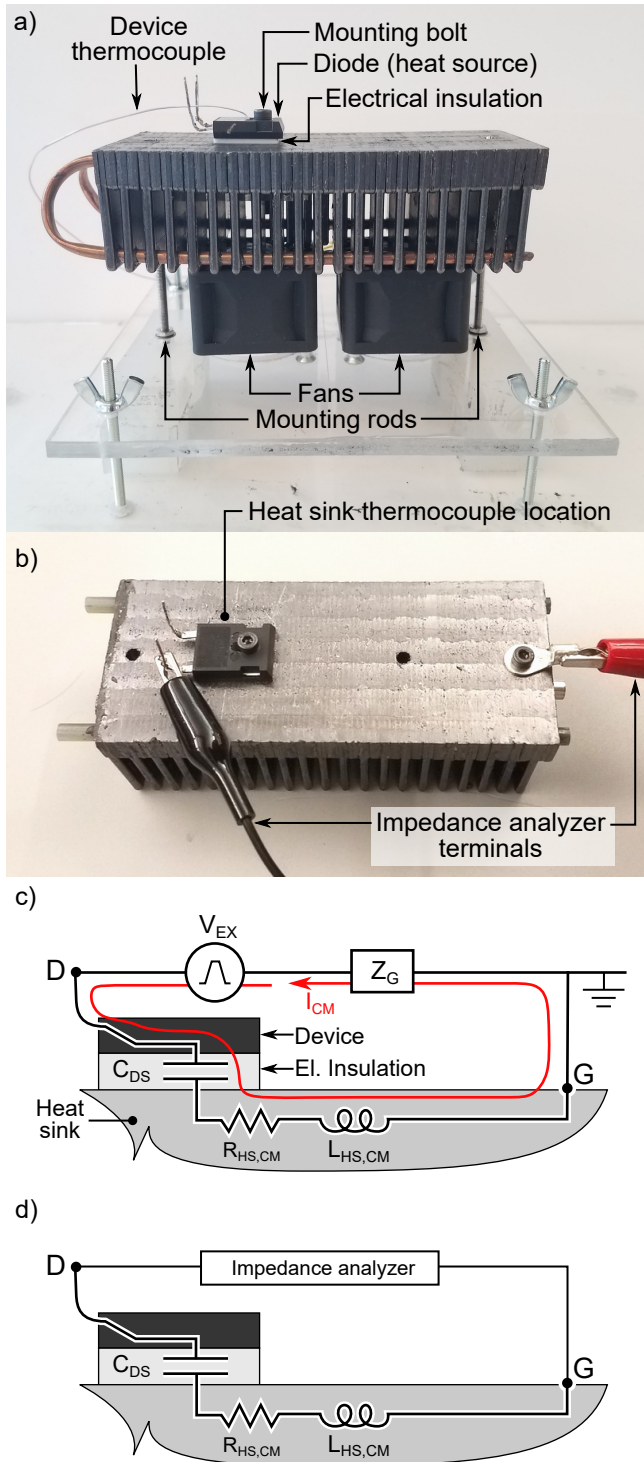
FIGURE 3. a) Thermal performance measurement setup, b) Impedance measurement setup, c) the equivalent circuit of common mode conducted emissions, and d) a schematic of the impedance measurement.

$R_{th,SA}$ is a sum of the conduction resistance within the heat sink and the convection resistance at the sink-air interface.

In all cases, the sink-to-ambient resistances of AL and NGS+HP heat sinks are comparable with a value of 0.4 $K \cdot W^{-1}$, while that of the NGS heat sink is approximately
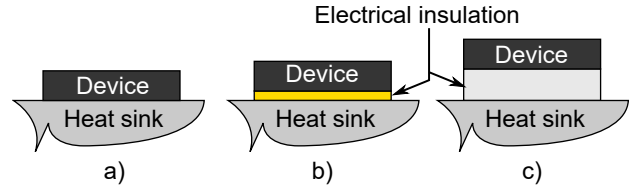

FIGURE 4. Measured cases: a) non-insulated direct mounting, b) polyimide film insulation, and c) Al_2O_3 insulating pad.

three times higher with a value of 1.2 $K \cdot W^{-1}$. The infrared camera images in Fig. **??** show that the low through–plane thermal conductivity of NGS limits the heat spreading in the base of the heat sink, which makes the right side of the heat sink inactive and, in turn, reduces the fin area that participates in the convective heat transfer. To make up for the decreased heat dissipation area, the temperature of the active portion of the heat sink must increase, which is visible by the hot spot in the NGS image.

The results of the cases with no electrical insulation show that the device-to-sink thermal resistance $R_{th,DS}$ of the NGS and NGS+HP heat sinks is the same as that of the AL heat sink with thermal grease, but 50 % lower than AL without thermal grease, which is attributed to the low hardness of NGS, which leads to better conformity and decreased TCR at the aluminum-NGS interface. Contrary to expectation, the same trend does not occur when the Al_2O_3 insulation pad is used. The measured device-to-sink resistance $R_{th,DS}$ of all three heat sinks when using the Al_2O_3 insulating pad is 2.5 $K \cdot W^{-1}$. Since the only difference in the three Al_2O_3 measurements is the TCR between the insulation pad and the heat sink, it can be inferred that the TCR at Al_2O_3-aluminum and Al_2O_3-NGS interfaces are comparable and the possibility to eliminate the need for a thermal grease seen in aluminum-NGS interfaces does not apply to Al_2O_3-NGS ones. To verify the latter finding, a study of TCR between Al_2O_3 and NGS using a specialized equipment would be necessary, but no such studies are available in the literature. The magnitude of TCR is a function of many geometrical, thermal, and mechanical parameters such as surface roughness, out-of-flatness, thermal conductivity, micro-hardness, and Young's modulus. Since most of these parameters have not been measured in this study, an explanation of the TCR behavior cannot be made.

When a polyimide film is used for electrical insulation, the device-to-sink thermal resistance $R_{th,DS}$ of the NGS and NGS+HP heat sinks is approximately 14 % lower than that of the AL one, which is a trend similar to but weaker than that in the non-insulated cases. Similar to the Al_2O_3 measurements, a physical explanation of the trend is not possible due to the high complexity of the TCR phenomenon, and a standalone study is recommended.

B. ELECTROMAGNETIC PERFORMANCE
The measured impedance of the common-mode emission path is shown in Fig. 7, where the top and bottom plots
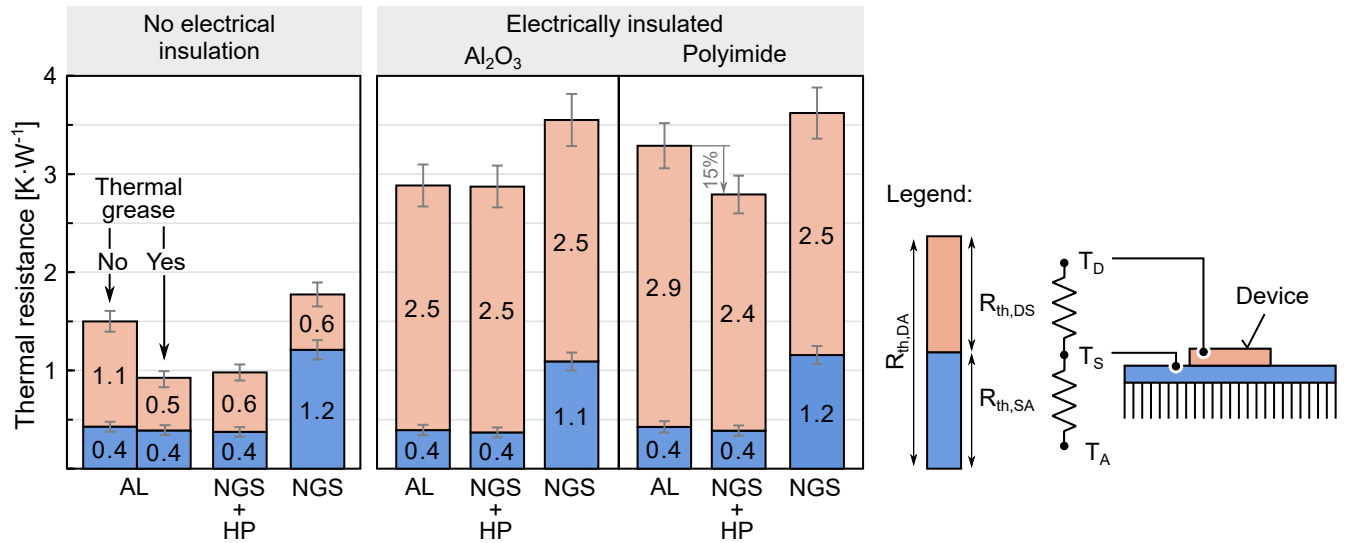
IEEE *Access*

FIGURE 5. The results of the thermal measurements. The total device-to-ambient thermal resistance $R_{th,DA}$ is represented by the total height of the stacked bars, and the de
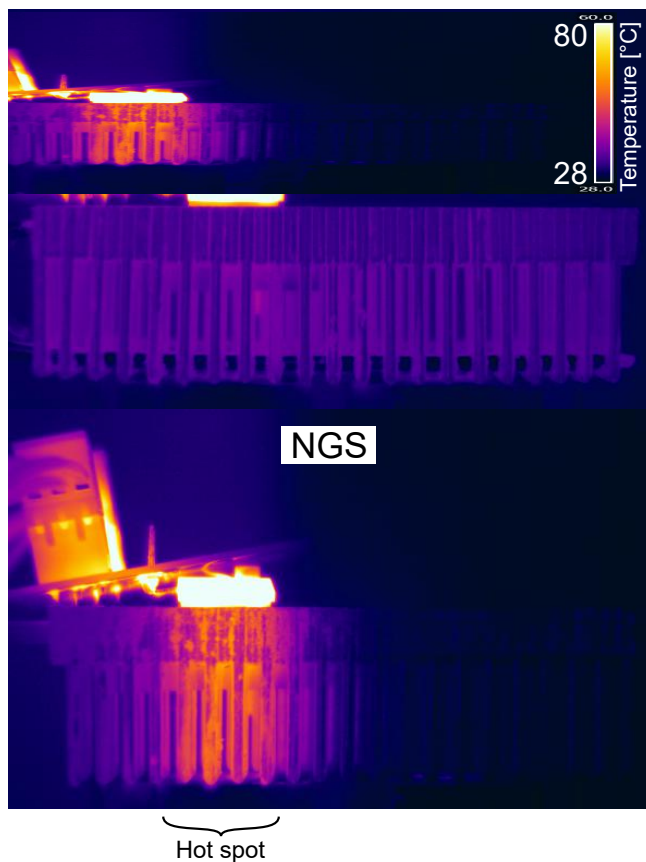
material has no effect on the impedance of the emissions path. The measurements of the non-insulated case show that the NGS and NGS+HP have higher impedance, but when electrical insulation is used, the total impedance is dominated by the C_{DS} capacitance. The latter conclusion is based on the $\theta = -90°$ phase and the linear decrease of the amplitude $|Z|$. The magnitude of the C_{DS} capacitance was determined from an equivalent series RLC circuit to be 23 pF for Al_2O_3 and 80 pF for the polyimide film.

IV. DISCUSSION

The potential of NGS heat sinks to reduce radiated emissions can be based on an analogy with antennas. As shown in Fig. 8a, a non-insulated ungrounded heat sink is conceptually identical to a monopole antenna. In antenna design, the radiation efficiency is a quantity that expresses the ratio of radiated and input energy. While antennas are designed for maximum radiation efficiency, a low value is desired for heat sinks to minimize the radiated emissions. Shahpari and Thiel [16] studied the effect of electrical conductivity on the radiation efficiency of antennas, and their results can be used for estimating the potential emission reduction of NGS heat sinks. Fig. 8b shows the radiation efficiency of two types of antennas as a function of the electrical conductivity. Based on the range of conductivities for aluminum, copper, and NGS that are highlighted by the gray zones, the potential emission reduction ranges from 12 % to 97 %. Besides the electrical conductivity, surface roughness has been reported to affect the radiation efficiency [17], [18]. Therefore, additional emission reduction might be possible due to the intrinsic surface roughness of NGS or the ability to easily manufacture NGS heat sinks with micrometer scale engineered surface features.

A validation of the emission reduction potential for geometrically complex heat sinks in practical applications can be

FIGURE 6. Infrared camera images of NGP+HP heat sink (top) and NGS heat sink (bottom). The poor heat conduction in the through–plane direction results in the hot spot in the NGS heat sink.

show the amplitude $|Z|$ and phase θ. The overlapping amplitude curves for the insulated cases imply that the heat sink
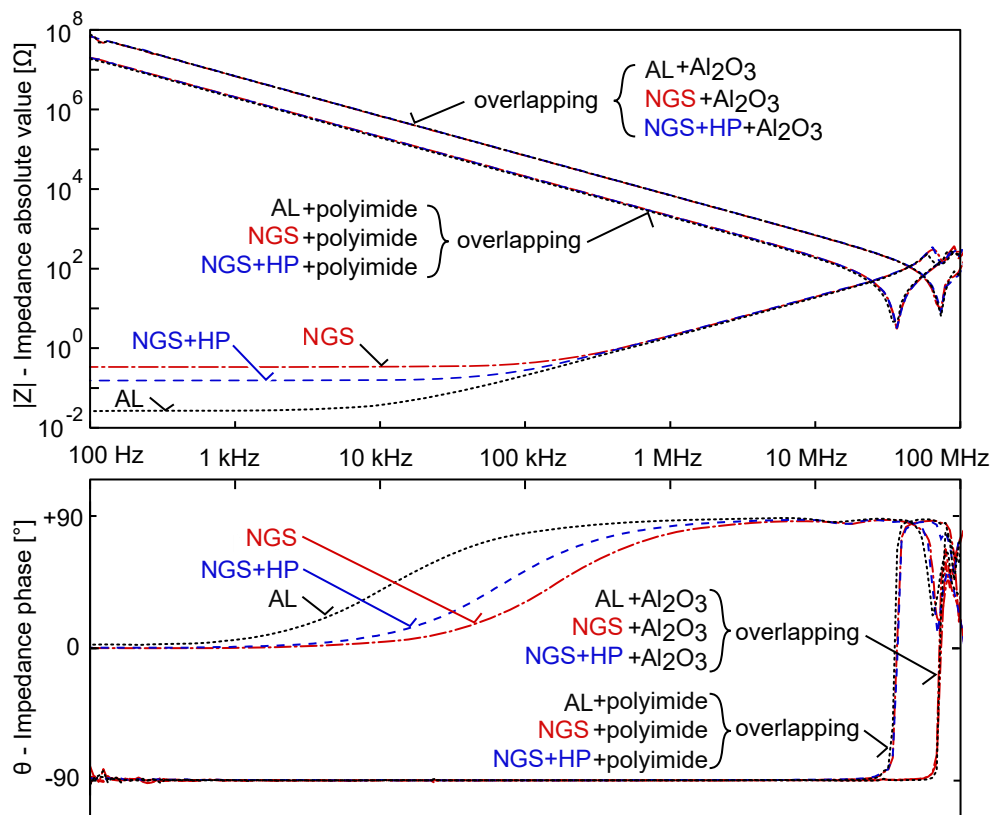
FIGURE 7. The results of impedance measurements with the amplitude $|Z|$ at the top and phase θ at the bottom.

done by numerical modelling and experimental work using a specialized equipment to capture the directional and near field/far field variation of the radiated spectrum. Building a numerical model is difficult due to the lack of electromagnetic properties of NGS. Attempts to measure the permittivity of NGS using an Agilent Technologies PNA-X network analyzer with the conventional probe were unsuccessful because the method is not suitable for anisotropic materials.

In our measurement of the common mode impedance, we showed that despite the two to four orders of magnitude lower electrical conductivity of NGS, a reduction in common mode emissions cannot be achieved for values of device-sink capacitance from 23 to 80 pF because the total impedance is dominated by the capacitive reactance. For significant emission reduction, the heat sink resistance would have to be equal to the capacitive reactance. Assuming a capacitance of 80 pF and a frequency of 1 MHz, the electrical conductivity of the heat sink would have to be in the order of 10 S·cm^{-1}, which is two orders of magnitude lower than the through–plane conductivity of NGS.

The thermal performance of the measured NGS+HP heat sink was shown to be comparable to the AL one, but it is necessary to note that the result is case dependent. For the present study we used two U shape heat pipes to show the best-case potential, but an optimized design can contain only a single straight heat pipe to reduce the complexity and cost.

The TCR at the interface between the heat pipe and heat sink is of concern as it can adversely affect the thermal performance. However, the present study showed that even with a low prototyping accuracy the heat pipes maintained good thermal contact with the heat sink and participated in the through–plane heat transfer.

To assist with evaluating the feasibility of NGS heat sinks for practical applications, a review of relevant findings has been compiled in Fig. 9. The focus has been narrowed down to NGS heat sinks with embedded heat pipes. In the non-insulated case, the good thermal performance of NGS heat sinks, which is equivalent to aluminum heat sinks with thermal grease, makes NGS an attractive choice, especially for weight-sensitive applications. In the present study the NGS+HP heat sink was 37 % lighter than the aluminum one. However, when considering replacing an existing aluminum heat sink with an NGS one, the weight reduction is determined by the selected density of NGS and the difference in heat sink geometry. The non-insulated case is relevant to LED lighting or power modules in which electrical insulation is not required or has been facilitated within the module packaging.

In the cases with electrical insulation, the thermal advantage of using NGS heat sinks diminishes as the possibility to eliminate the thermal grease no longer exists. Additional measurements, which have not been included in Fig. 5 and
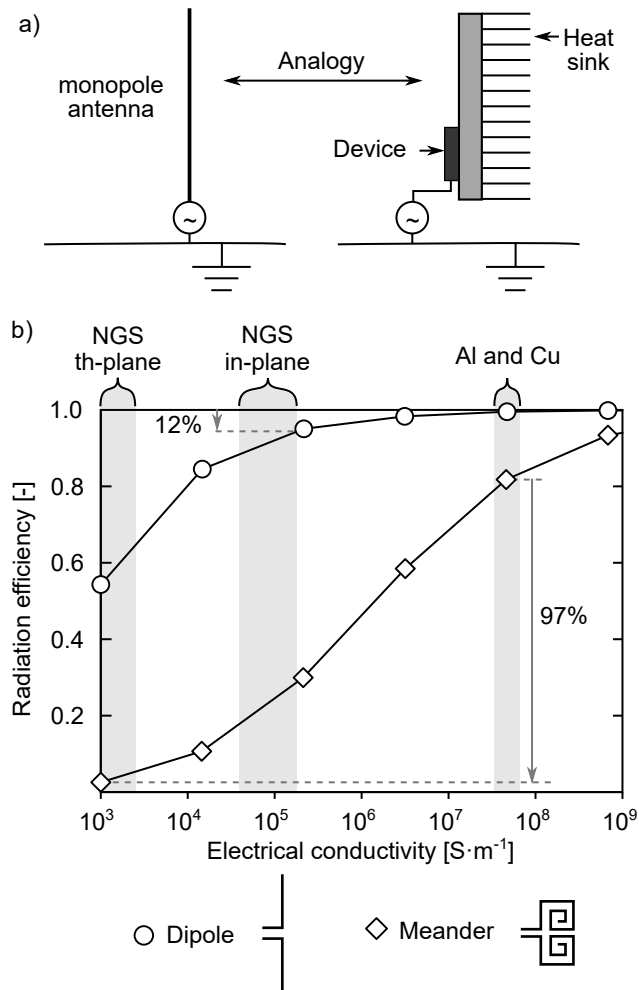
IEEE *Access*

FIGURE 8. a) an illustration of the analogy between an antenna (monopole) and ungrounded heat sinks, and b) the radiation efficiency of dipole and meander antennas as a function of the electrical conductivity (data by Shahpari and Thiel [16]).

FIGURE 9. A comparison of the thermal resistance, device-to-sink capacitance C_{DS}, and weight of the measured cases.

9, indicate that by applying a thermal grease to the device-Al_2O_3 and Al_2O_3-sink interfaces, the device-to-sink thermal resistance is reduced by 64 % making this configuration the best in terms of the thermal performance. The reduction is in agreement with the results in [19]. While it is possible to use a thermal grease with NGS heat sinks, this case has not been investigated here. The low parasitic capacitance of the thick Al_2O_3 insulation pad is favorable for a reduction of common mode conducted emissions. The potential weight reduction is identical to the non-insulated case because the weight of the insulation is much lower in comparison to the heat sinks. For very small heat sinks, the relatively high Al_2O_3 density of approximately 3.8 g·cm^{-3} can make the polyimide tape a lighter alternative.

While the present study shows the potential benefits of using NGS heat sinks, the assumption of identical geometry is not relevant for practical heat sink considerations as the difference in material properties results in a different optimal geometry for metal 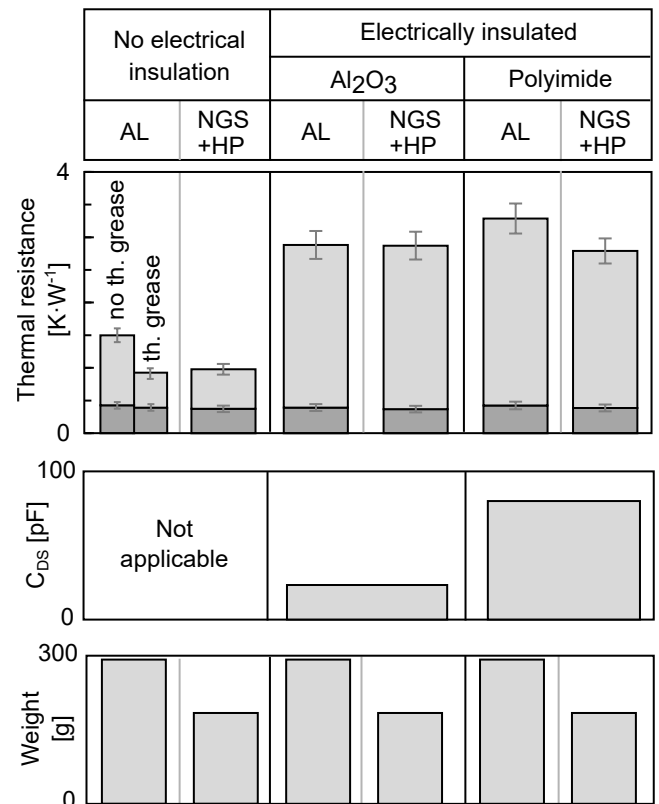and NGS heat sinks. To fully explore the thermal and weight improvements, case-specific optimization studies must be carried out by adopting approaches similar to those described by Wu et al. [20] or Dede et al. [21] and using the NGS material properties reported in [2]. The optimization can be targeted to either minimizing the weight while keeping the thermal resistance below a required value or minimizing the thermal resistance while respecting the characteristics of the available fan and keeping the dimensions within the limits. To reduce the cost and complexity, the designs with heat pipes can be penalized to force the optimization algorithm to choose options that do not require heat pipes, if such possibility exists. The difference in optimal geometry of metal and NGS heat sinks was illustrated in Figure 10. The anisotropy in thermal conductivity, which is symbolized by the arrows, is reflected in the optimal heat sink dimensions. Using fewer fins with larger dimensions can lead to the same performance without the need to use heat pipes. An example of a simple parallel plate heat sink was chosen for Figure 10 but the NGS technology allows using an arbitrary fin shape. Similar to 3D printing, which makes manufacturing of complex heat sink shapes possible, the laminated design of NGS heat sinks allows for manufacturing geometries that were previously impossible or cost prohibitive.

The main known drawback of NGS heat sinks is the low mechanical strength. In the in–plane direction, the tensile
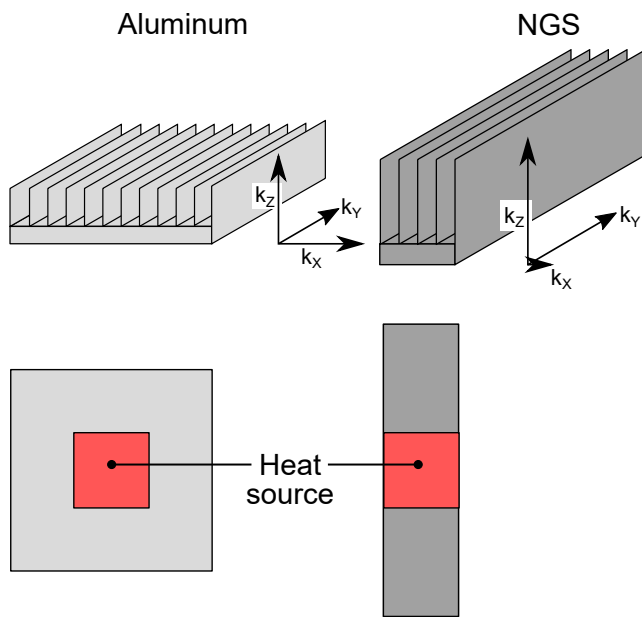
FIGURE 10. An illustration of the different optimal heat sink geometry for anisotropic metals and NGS.

strength of NGS is only 0.4 to 4.8 % that of 6061 aluminum. Impregnating NGS with a polymer improves the mechanical strength, but the effect of impregnation on other NGS properties should be studied. Other open research questions include measuring and understanding the TCR between NGS and other surfaces such as metals or plastics; validation of the potential to reduce radiated emissions; and investigating the long-term degradation under cyclic conditions or in a harsh environment.

V. CONCLUSIONS

The thermal and electromagnetic performance, the feasibility, and the need for future research of natural graphite sheet (NGS) heat sinks were addressed. The thermal measurements showed that by embedding heat pipes into NGS heat sinks, the low through–plane thermal conductivity can be mitigated, and the resulting heat sink thermal resistance is the same as that of a geometrically identical aluminum heat sink. The device-to-sink thermal resistance of NGS heat sinks with no electrical insulation is identical to that of aluminum heat sinks with thermal grease, offering cost and reliability benefits. For the electrically insulated cases, the advantages of using NGS heat sinks decrease or diminish, and further research is needed to explain the measured trends. No improvement in thermal performance was seen for Al_2O_3 insulating pads, and only 15 % reduction in the device-to-ambient thermal resistance can be achieved when using adhesive-coated polyimide insulation.

Despite the four orders of magnitude lower electrical conductivity, NGS heat sinks cannot reduce the common mode conducted emissions because the total impedance of the common mode current path is dominated by the parasitic

device-to-sink capacitance. To achieve a significant reduction in common mode emissions, the electrical conductivity of a heat sink material would have to be in the order of 10^{-1} S·cm^{-1}, which is two orders of magnitude lower than the low through–plane conductivity of NGS. The potential for a reduction of radiated emissions was quantified to be 12 to 97 % based on an analogy with antennas. A combination of numerical, experimental, and material characterization work is suggested to validate this prediction.

NGS heat sinks are a feasible option for weight sensitive applications, especially in cases where no electrical insulation is required. To fully utilize the potential for good thermal performance and low weight, a case specific optimization of the heat sink shape based on a numerical model coupled with state-of-the-art optimization algorithms is recommended. The low mechanical strength of NGS must be taken into account when designing the heat sink and its clamping mechanism.
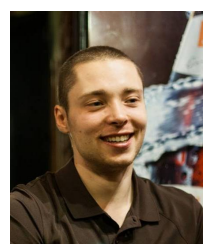
REFERENCES

[1] U.S. Geological Survey, "Mineral commodity summaries 2019: U.S. Geological Survey," 2019.

[2] M. Cermak, N. Perez, M. Collins, and M. Bahrami, "Material properties and structure of natural graphite sheet," 2020. Manuscript in preparation.

[3] W. Jiang, G. Nadeau, K. Zaghib, and K. Kinoshita, "Thermal analysis of the oxidation of natural graphite — effect of particle size," Thermochimica Acta, vol. 351, no. 1, pp. 85 – 93, 2000.

[4] E. Levy, H. Bilirgen, and J. Dupont, "Recovery of water from boiler flue gas using condensing heat exchanger," tech. rep., Energy Research Center, Lehigh University, 2011.

[5] S. C. Chelgani, M. Rudolph, R. Kratzsch, D.Sandmann, and J.Gutzmer, "A Review of Graphite Beneficiation Techniques," Mineral Processing and Extractive Metallurgy Review, vol. 37, no. April, pp. 58–68, 2016.

[6] A. Pizza, R. Metz, M. Hassanzadeh, and J.-L. Bantignies, "Life cycle assessment of nanocomposites made of thermally conductive graphite nanoplatelets," The International Journal of Life Cycle Assessment, vol. 19, pp. 1226–1237, Jun 2014.

[7] G. Chen, J. Capp, G. Getz, D. Flaherty, and J. Norley, "Optimum Design of Heat Sinks Using Non-Isotropic Graphite Composites," in ASME 2003 Heat Transfer Summer Conference Heat Transfer: Volume 3, pp. 489–494, ASME, 2003.

[8] E. E. Marotta, M. J. Ellsworth, J. Norley, and G. Getz, "The Development of a Bonded Fin Graphite/Epoxy Heat Sink for High Performance Servers," 2003 International Electronic Packaging Technical Conference and Exhibition, Volume 2, pp. 139–146, 2003.

[9] T. Icoz and M. Arik, "Light weight high performance thermal management with advanced heat sinks and extended surfaces," IEEE Transactions on Components and Packaging Technologies, vol. 33, pp. 161–166, March 2010.

[10] M. Cermak, J. Kenna, and M. Bahrami, "Natural-graphite-sheet based heat sinks," in 2017 33rd Thermal Measurement, Modeling Management Symposium (SEMI-THERM), pp. 310–313, March 2017.

IEEE *Access*

[11] M. Cermak, W. J. He, and M. Bahrami, "A transient thermal tester as an alternative to thermocouples for characterizing heat sinks," in 2018 34th Thermal Measurement, Modeling Management Symposium (SEMI-THERM), pp. 148–154, March 2018.

[12] I. Grobler and M. N. Gitau, "Analysis, modelling and measurement of the effects of aluminium and polymer heatsinks on conducted electromagnetic compatibility in dc–dc converters," IET Science, Measurement Technology, vol. 11, no. 4, pp. 414–422, 2017.

[13] A. Bhobe, H. Chu, L. Comiskey, X. Jiao, and X. Li, "Thermal and emi performance of composite plastic molded heat sinks and hybrid tim materials," International Symposium on Microelectronics, vol. 2014, no. 1, pp. 000222–000228, 2014.

[14] M. Cermak, Natural graphite sheet heat sinks for power electronics. PhD thesis, Simon Fraser University, 2020. In preparation.

[15] M. Cermak, X. Faure, A. Saket, M. Ordonez, and M. Bahrami, "Natural graphite sheet heat sinks with embedded heat pipes - dataset." https://dx.doi.org/10.20383/101.0213, 2020.

[16] M. Shahpari and D. V. Thiel, "The impact of reduced conductivity on the performance of wire antennas," IEEE Transactions on Antennas and Propagation, vol. 63, pp. 4686–4692, Nov 2015.

[17] D. Shamvedi, O. J. McCarthy, E. O'Donoghue, P. O'Leary, and R. Raghavendra, "Improved performance of 3d metal printed antenna through gradual reduction in surface roughness," in 2017 International Conference on Electromagnetics in Advanced Applications (ICEAA), pp. 669–672, Sep. 2017.

[18] C. R. Garcia, R. C. Rumpf, H. H. Tsang, and J. H. Barton, "Effects of extreme surface roughness on 3D printed horn antenna," Electronics Letters, vol. 49, no. 12, pp. 734–736, 2013.

[19] M. Garcia-Poulin, M. Ahmadi, M. Bahrami, E. Lau, and C. Botting, "Thermal resistance of electrical insulation for bolted and clamped discrete power devices," in 2018 34th Thermal Measurement, Modeling Management Symposium (SEMI-THERM), pp. 176–180, March 2018.

[20] T. Wu, B. Ozpineci, M. Chinthavali, Z. Wang, S. Debnath, and S. Campbell, "Design and optimization of 3D printed air-cooled heat sinks based on genetic algorithms," 2017 IEEE Transportation and Electrification Conference and Expo, ITEC 2017, pp. 650–655, 2017.

[21] E. M. Dede, S. N. Joshi, and F. Zhou, "Topology Optimization, Additive Layer Manufacturing, and Experimental Testing of an Air-Cooled Heat Sink," Journal of Mechanical Design, vol. 137, 10 2015. 111403.

MOHAMMAD ALI SAKET (S'15) received the B.Sc. degree in electrical engineering from the Amirkabir University of Technology, Tehran, Iran, in 2009, and the M.Sc. degree in power electronics from the Sharif University of Technology, Tehran, Iran, in 2011. He is currently working toward the Ph.D. degree at the University of British Columbia, Vancouver, BC, Canada. His research interests include planar magnetic, integrated magnetic structures, AC/DC and DC/DC converters, resonant converters, applications of FEA in power electronics, EMI, and Wireless Power Transfer.

MARTIN CERMAK received both his bachelor's degree in mechanical engineering and master's degree in process engineering from Brno University of Technology, Czech Republic. He worked as a fluid dynamics and heat transfer engineer at Skoda Transportation, and currently he is finishing his PhD research on natural graphite sheet heat sinks at Simon Fraser University, Canada. Martin is interested in, and motivated by, working on pressing environmental and societal issues that require collaborative and multi-disciplinary research.

XAVIER FAURE is a Master's student graduating in the fields of environmental and energy engineering at the INSA Lyon, France. He worked as an intern for 20 weeks at the Simon Fraser University, Canada, under the supervision of Martin Cermak. He is currently completing an end-of-studies internship in Citrus Engineering, Mexico in the field of energy efficiency and solar heat utilization for industry. He aspires to work for a sustainable future in the field of energy engineering and its efficient utilization.

MARTIN ORDONEZ (S02M09) was born in Neuquen, Argentina. He received the Ing. degree in electronics engineering from the National Technological University, Cordoba, Argentina, in 2003, and the M.Eng. and Ph.D. degrees in electrical engineering from the Memorial University of Newfoundland (MUN), St. John's, NL, Canada, in 2006 and 2009, respectively.

He is currently the Canada Research Chair in Power Converters for Renewable Energy Systems and Professor with the Department of Electrical and Computer Engineering, University of British Columbia, Vancouver, BC, Canada. He is also the holder of the Fred Kaiser Professorship on Power Conversion and Sustainability at UBC. He was an adjunct Professor with Simon Fraser University, Burnaby, BC, Canada, and MUN.

His industrial experience in power conversion includes research and development at Xantrex Technology Inc./Elgar Electronics Corp. (now AMETEK Programmable Power in San Diego, California), Deep-Ing Electronica de Potencia (Rosario, Argentina), and TRV Dispositivos (Cordoba, Argentina). With the support of industrial funds and the Natural Sciences and Engineering Research Council, he has contributed to more than 140 publications and R&D reports.

Dr. Ordonez is a Guest Editor for IEEE JOURNAL OF EMERGING AND SELECTED TOPICS IN POWER ELECTRONICS, Associate Editor of the IEEE TRANSACTIONS ON POWER ELECTRONICS, and Editor for IEEE TRANSACTIONS ON SUSTAINABLE ENERGY. He serves on several IEEE committees, and reviews widely for IEEE/IET journals and international conferences. He was awarded the David Dunsiger Award for Excellence in the Faculty of Engineering and Applied Science (2009) and the Chancellors Graduate Award/Birks Graduate Medal (2006), and became a Fellow of the School of Graduate Studies, MUN.

DR. MAJID BAHRAMI is a Professor of Mechanical Engineering and Tier 1 Canada Research Chair in Alternative Energy Conversion Systems at SFU. He is a Fellow of the Canadian Academy of Engineers (FCAE) and the American Society of Mechanical Engineers (FASME). Bahrami championed interdisciplinary, collaborative research in multitudes of sustainable clean energy systems, including: harvesting and transforming low-grade heat for sustainable air conditioning, thermal energy storage, desalination, heat pump systems and dehumidification for applications in automotive, agri-food, sustainable city, and thermal hybrid microgrids. He has a strong track record in successful collaboration with national and international research institutes and industry. He formed 2 start-ups; won national and international research and innovation awards; published 8 patents and 300+ publications; and supervised 120+ highly qualified personnel, including 5 professors.

● ● ●